Chemosensory Adaptation In an Electronic Nose

R. Gutierrez-Osuna[†], N. Powar and P. Sun
Department of Computer Science and Engineering
Wright State University
Dayton, OH 45435

Abstract

This article presents a computational mechanism inspired by the process of chemosensory adaptation in the mammalian olfactory system. The algorithm operates on multiple subsets of the sensory space, generating a family of discriminant functions for different volatile compounds. A set of selectivity coefficients is associated to each discriminant function on the basis of its behavior in the presence of mixtures. These coefficients are employed to form a weighted average of the discriminant functions and establish a feedback signal that reduces the contribution of certain sensory inputs, inhibiting the overall selectivity of the system to previously detected analytes. The algorithm is validated on a database of organic solvents using an array of temperature-modulated metal-oxide chemoresistors.

1 Introduction

The integration of gas sensor arrays and pattern analysis algorithms has received much attention in recent years as an effective, low-cost alternative to odor measurement, conventionally carried out with analytical instruments or human panels [1]. The broad and overlapping selectivity of gas sensors can be utilized to characterize a wide range of odors by processing the multivariate fingerprint of volatile compounds across a sensor array. Pattern-recognition algorithms can then be used as an alternative to chemical analysis to solve problems such as odor classification, multi-component regression, or exploratory data visualization.

This article briefly reviews the process of signal processing in the mammalian olfactory pathway and proposes a computational mechanism that mimics the effects of olfactory adaptation. The method is inspired, at the functional level, by the roles of glomeruli in the olfactory bulb and centrifugal feedback from the olfactory cortex. In addition, we implement a hardware excitation procedure that can be employed to perform active sensing on commercial sensors. The proposed computational and instrumentation mechanisms are experimentally validated on a sensor array consisting of four temperature-modulated metal-oxide chemoresistors using two organic solvents and their mixture.

[†] Corresponding author (rgutier@cs.wright.edu).

2 Review of the olfactory pathway

The mammalian olfactory system can be divided into three basic subsystems [2]: olfactory epithelium, olfactory bulb and olfactory cortex. The computational pathway that serves as a model to this work is shown in Figure 1. Volatile compounds entering the nostrils are detected in the olfactory epithelium by a large number (10-100 million) of olfactory neurons [3]. Bundles of olfactory neuron axons access the brain via the cribiform plate, relaying their information to the mitral and tufted cells in the olfactory bulb through spherical clusters of synapses called glomeruli. Nearly 25,000 receptor axons converge to each glomerulus, which in turn connects to approximately 25 mitral cells and 70 tufted cells. The olfactory bulb presents a number of local microcircuits, mediated by periglomerular and granule cells, which perform complex excitatory and inhibitory functions at the glomeruli and mitral/tufted levels, respectively [4, 5, 6]. Mitral/tufted axons form the lateral olfactory tract, which transmits olfactory information to the olfactory cortex. The main target of the lateral olfactory tract is a collection of cortical regions in the brain collectively called the primary olfactory cortex. Among those regions, the piriform cortex is the largest area and plays a central role in the conscious recognition of odors. In addition, the lateral olfactory tract is heavily interconnected with the limbic system, which explains the effects of smell on emotions and mood. Finally, the olfactory cortex sends centrifugal inputs back to the olfactory bulb (primarily to the granule layer), resulting in a complex feedback mechanism that is believed to play a central role in olfactory adaptation [7, 8].

Detection of odorant molecules is performed by protein binding at the cilia of the olfactory neurons. The pioneering work of Buck and Axel [10] has lead to the identification of a family of approximately 1,000 receptor proteins that are responsible for this molecular detection process. Malnic et al. [9] have also confirmed that each of these receptor proteins can identify multiple odorants and that each odorant is, in turn, identified by multiple

receptor proteins, leading to an odor encoding mechanism based on a combinatorial coding of olfactory receptors. In addition, each olfactory neuron appears to be dedicated to a particular olfactory receptor, and neurons expressing the same receptor converge onto single or a small subset of glomeruli in the olfactory bulb [11]. These findings confirm a forty-year-old hypothesis [4], according to which glomeruli act as functional units or "labeled lines" for a subset of odorant molecules. Additional evidence indicates that odor quality may be encoded in spatial patterns in the olfactory epithelium and the glomerular layer [12, 13], whereas odor intensity would be encoded in the number of active receptors [14]. Considering the cross-selectivity of olfactory receptor proteins and the high convergence ratio from receptors to glomeruli, it can be concluded that biological olfactory transduction is based on the principles of high redundancy and partial specificity [4].

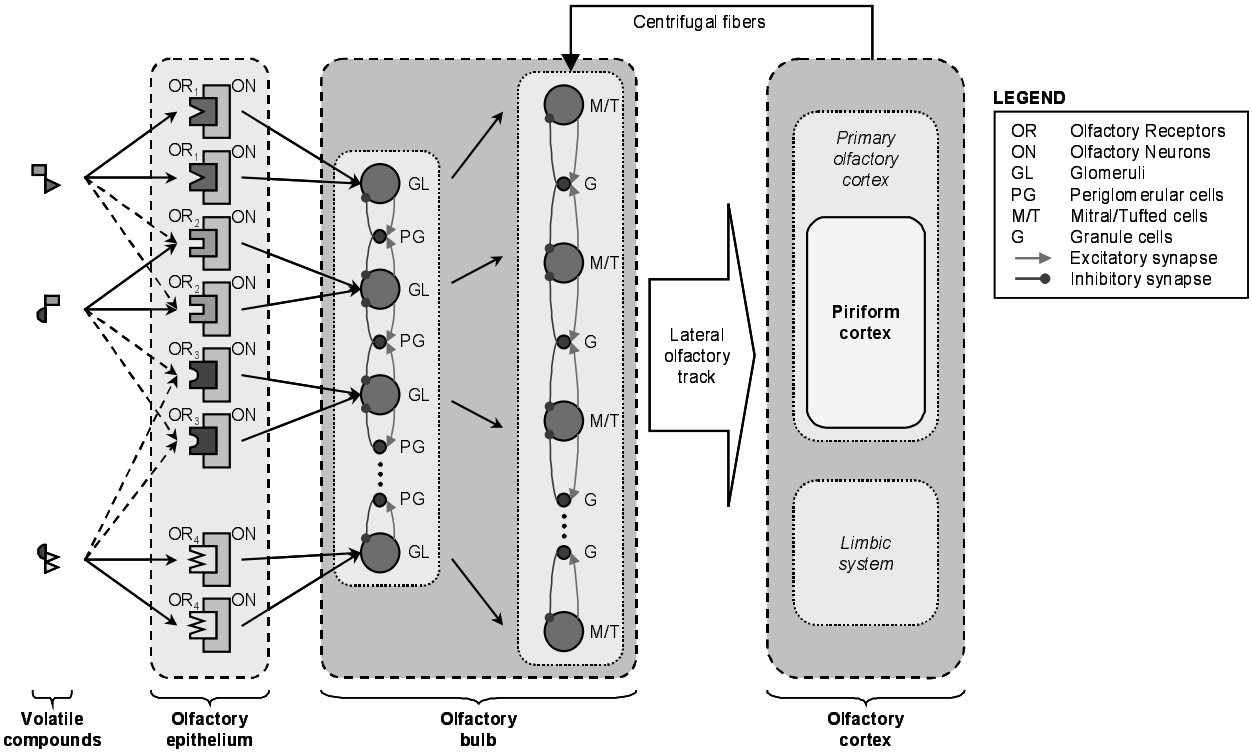

Figure 1. Computational model of the olfactory pathway (adapted from [3, 9])

3 An approach for mimicking chemosensory adaptation

The algorithm presented in this article is inspired by the aforementioned model of olfactory processing and adaptation in the biological system. We borrow, in particular, the concepts of glomeruli as labeled lines that detect specific odors, and the modulation of bulbar activity through centrifugal fibers for the purpose of olfactory adaptation. Our approach is depicted in Figure 2. Sensory inputs with similar selectivity profiles are grouped in bundles $s^{(k}$ and passed to a family of discriminant functions $g_c^{(k}$, one for each odor class ω_c, such that:

$$g_c^{(k}\left(s^{(k}\right)=\begin{cases}1 & s\in\omega_c\\ -1 & s\notin\omega_c\end{cases} \qquad (1)$$

Our current implementation computes a set of linear discriminant functions of the form $g_c^{(k}\left(s^{(k}\right)=G_c^{(k}s^{(k}+H_c^{(k}$ using the least-squares minimization criterion:

$$\left[G_c^{(k},H_c^{(k}\right]=\underset{G,H}{\arg\min}\left[\sum_{\forall s}\left(Gs^{(k}+H-g_c^{(k}\left(s^{(k}\right)\right)^2\right] \qquad (2)$$

Information from these discriminant functions is combined in a higher processing layer to determine the identity of the odor. In our algorithm, this is accomplished by computing a cumulative discriminant function $g_c(s)$ that performs a weighted average of the discriminant functions from all sensor bundles of any given class:

$$g_c(s)=\frac{\sum_k f\left(g_c^{(k}\left(s^{(k}\right)\right)w_c^{(k}\left(1-i^{(k}\right)}{\sum_k w_c^{(k}} \qquad (3)$$

where $s=[s^{(1},s^{(2},s^{(3},...]$, $w_c^{(k}$ is a weighting coefficient that measures the selectivity of sensory bundle $s^{(k}$ to odor class ω_c, and $i^{(k}$ is an inhibitory term to excite/depress the selectivity of the system to specific odors. The term $\sum_k w_c^{(k}$ in the denominator is used to normalize the response relative to the overall sensitivity of the sensor array to each odor. Finally, the transform $f(\cdot)$ is a squashing sigmoidal function that limits the activation level of the discriminant functions in the range [0,1]:

$$f(x)=\frac{1}{2}(\tanh(x)+1) \tag{4}$$

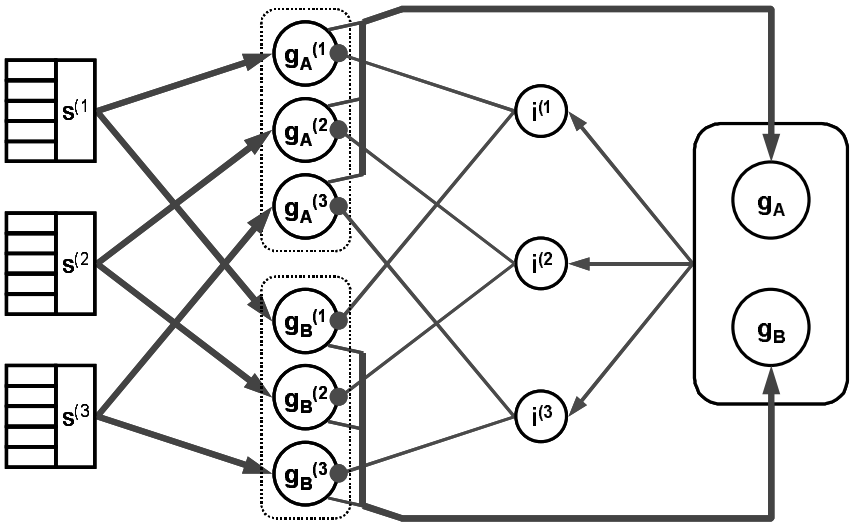

Figure 2. Structure of the proposed algorithm with sensory bundles $s^{(k}$, discriminant functions $g_c^{(k}$, cumulative discriminants g_c and inhibitory feedback $i^{(k}$

3.1 Determining the selectivity and inhibitory terms

The rationale for using the selectivity coefficients $w_c^{(k}$ is to weight the contribution of each discriminant function $g_c^{(k}$ in direct proportion to its specificity for odor class ω_c. This is measured by computing the average detection level of the discriminant function $g_c^{(k}$ to input mixtures s_{c^+}, where the term c^+ denotes input mixtures containing analyte ω_c *plus* others. The weighting coefficients are therefore estimated as:

$$w_c^{(k}=E\left[g_c^{(k}\left(s_{c^+}^{(k}\right)\right]_{\forall c^+} \tag{5}$$

The inhibitory term $i^{(k}$ is computed by feeding back the cumulative discriminant level for each odor $g_c(s)$, properly scaled and normalized by the selectivity coefficients $w_c^{(k}$:

$$i^{(k}(s)=\tanh\left(\lambda\frac{\sum_c g_c(s)w_c^{(k}}{\sum_c w_c^{(k}}\right) \tag{6}$$

where the term $g_c(s)$ serves as an indicator variable for the presence of odor ω_c and the coefficient λ can be used to drive the inhibitions to saturation. These inhibitory terms will reduce the contribution of sensory bundles $s^{(k}$ according to their selectivity towards previously detected odors.

4 Temperature-modulation for metal-oxide chemoresistors

Among the various technologies that have been used for odor sensors [1], metal-oxide (MOX) chemoresistors are widely employed due to their commercial availability and simple interface [15]. Despite their popularity, MOX sensors present poor specificity. Besides physical or chemical modification of the sensors (e.g. geometry, catalysts), three basic approaches can be employed to improve the selectivity of MOX-based instruments: (*i*) sample preparation with analytical-chemistry procedures such as thermal desorption or chromatography [16, 17], (*ii*) computational analysis of the sensor transient response patterns [18, 19] and (*iii*) advanced instrumentation procedures such as AC impedance spectroscopy or temperature modulation [20, 21, 22].

Temperature-modulation approaches are based on the fact that the selectivity of MOX sensors is greatly influenced by its operating temperature, since the reaction rates for different volatile compounds and the stability of adsorbed oxygen species are a function of surface temperature [23]. This temperature-selectivity dependence can therefore be exploited to improve the selectivity of MOS sensors by cycling the operating temperature during exposure to volatile compounds and subsequently processing the dynamic response of the sensor. In a previous article [24] we have reported significant selectivity enhancements on temperature-modulated Taguchi-type MOX sensors [25]. The sensors were driven with a low frequency (0.125Hz-4Hz) sinusoidal heater voltage of 0-7V amplitude. It was concluded that, due to thermal inertia, lower excitation frequencies were necessary to resolve dynamic information at multiple temperatures.

In this article we extend the previous approach by exciting the sensors at various temperature ranges using the heater-voltage profile shown in Figure 3. This profile contains six sinusoidal segments with a 1-6V DC offset in increments of 1V. At each segment, five sinusoidal cycles with an amplitude of 2V and a period T=20s are generated. In order to eliminate the initial thermal transient response, only the last cycle of each segment is used for pattern analysis [26]. One of the long-term goals of our research is active sensing, for which it is essential that the dynamic features are independent of the recent thermal history of the sensor. It is expected that the proposed instrumentation procedure will allow us to perform active sensing by driving each sensor at a single temperature range, and actively changing these temperature ranges to reduce the sensitivity to previously detected odors.

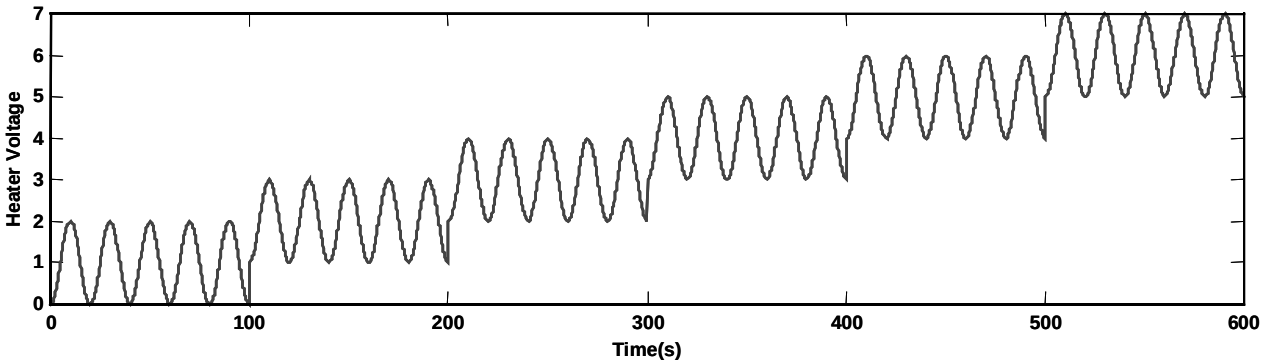

Figure 3. Heater voltage profile for the metal-oxide sensors

5 Experimental results

To verify the feasibility of our approach we have collected an experimental dataset using an array of four Figaro sensors (2602, 2610, 2611, 2620). The sensors were mounted on the cap of a 30 ml vial containing 10 ml of analytes. Acetone (odor A), ethanol (odor B) and a 50/50 mixture of these two analytes were employed in this study. The resistance of the sensors was measured at 10 samples/second using voltage dividers connected to a LabVIEW-driven data acquisition card. Fifteen samples per odor were collected over a period of five days. The average response of the four sensors vs. the cyclic heater voltage is shown in Figure 4. Only the fifth cycle of each segment is plotted. It can be observed that, although the sensors have overlapping selectivities, they respond differently to the analytes at the various temperature ranges. Notice the unique pattern of sensor 4 in the 5-7V, which clearly discriminates acetone from ethanol. Of particular significance is the behavior of the 50/50 mixture on the different sensors and temperature ranges. Interestingly, the mixture generates a pattern similar to acetone on sensor 1 (practically identical on the 3-5V range) but similar to ethanol on the other three sensors. This behavior is critical to the success of our approach because it allows the system to bias its selectivity by favoring certain sensors and temperature ranges.

In order to evaluate the performance of our approach, we extract a number of features from each of the sensors and temperature ranges. Looking at the cyclic patterns of Figure 4, one may consider several features, including the vertical center of gravity, the area enclosed by the curve and the orientation of the principal axes. In this article, however, we employ a simpler non-parametric approach that consists of sub-sampling the sensor response (on the fifth cycle) down to 10 samples. With four sensors and six temperature ranges, this yields twenty-four 10-dimensional feature vectors (or sensor bundles), which are used to obtain the linear discriminant functions $g_c^{(k}$ (k=1-24; c=1,2).

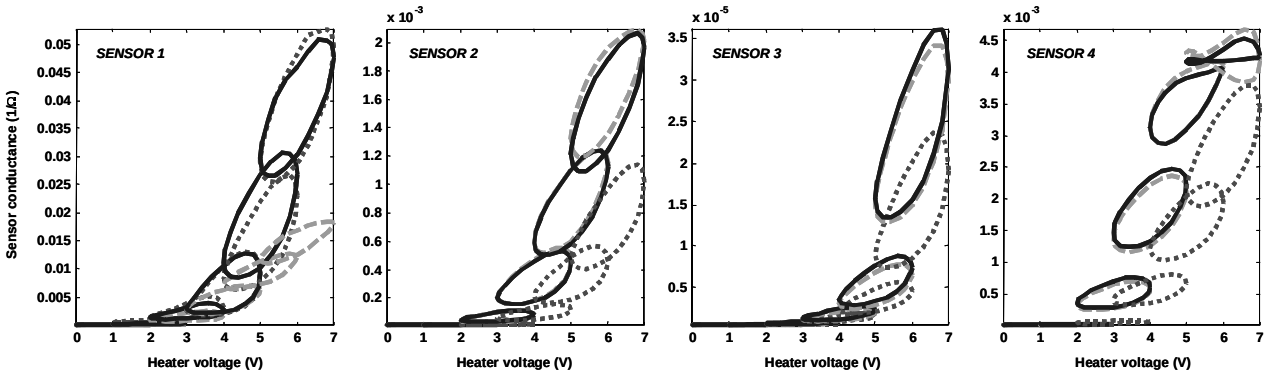

Figure 4. Sensor conductance versus cyclic heater voltage for acetone (dotted), ethanol (dashed) and 50/50 mixture (solid)

The regression matrices $\left(G_A^{(k}, H_A^{(k}\right)$ are trained using pure acetone, whereas $\left(G_B^{(k}, H_B^{(k}\right)$ are obtained from the pure ethanol samples. The mixture samples are used to determine the selectivity coefficients $w_c^{(k}$. The results are shown in Figure 5, where the inhibitory terms $i^{(k}$ have been set to zero to reflect that no odor has been detected previously. Each row denotes an example and each column a discriminant function. The first 15 rows correspond to acetone samples, the next 15 rows correspond to ethanol samples and the last 15 rows are for the 50/50 mixture. Columns 1-24 correspond to the discriminant functions for the first odor class. Columns 1-6 are associated to the response of sensor 1 on the 0-2V, 1-3V, up to 5-7V heater voltage range, respectively. Columns 7-12 are for sensor 2, and so forth.

Several conclusions can be extracted from these results. First, the linear discriminant functions can clearly identify the individual analytes: the $f\left(g_A^{(k}\right)$ block responds selectively to acetone but not to ethanol, whereas the $f\left(g_B^{(k}\right)$ block responds mostly to ethanol. Second, the response of the sensors at low temperature (0-2V, 1-3V) is not discriminative, as illustrated by the response of columns 1, 7, 8, 13, etc. Third, the discriminant functions have a diverse response to the 50/50 mixture (rows 31-45). Columns 3-6 are high and columns 27-30 are low, indicating that the corresponding discriminants would classify these samples as acetone. The reverse classification occurs with the remaining columns. All these results are consistent with the structure of the cyclic patterns previously shown in Figure 4.

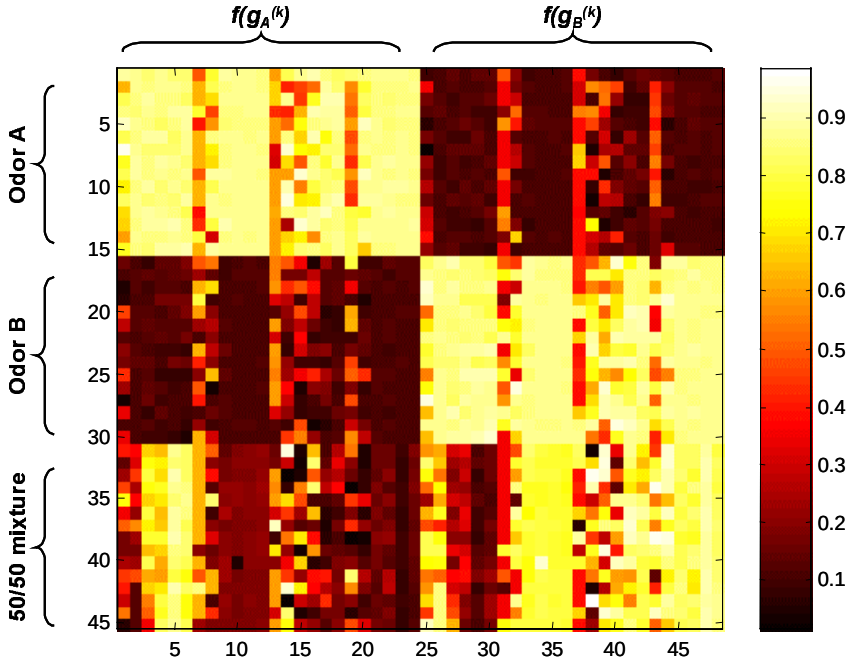

Figure 5. Activation level of the linear discriminant functions

We finally test the ability of this algorithm to mimic chemosensory adaptation by analyzing the activation level of the cumulative discriminant functions $g_c(s)$ after the system has identified each of the pure analytes and set the inhibitory terms $i^{(k}$ accordingly. A value of $\lambda=10$ is used in equation (6). The results are illustrated in Figure 6. In the absence of adaptation, as shown in Figure 6(a), the cumulative discriminants $g_c(s)$ present a high level when $s \in \omega_c$ and a low level otherwise. The 50/50 mixture induces a high activation pattern on both cumulative discriminants, although $g_B(s)$ dominates since the mixture is closer to odor B on three out of the four sensors and, therefore, more discriminant functions $g_B^{(k}$ become activated. When the system adapts to odor A (Figure 6(b)), the activation level of $g_A(s)$ drops significantly for all samples, including those from class A. As a result, the activation pattern for the 50/50 mixture becomes similar to that of odor B. Conversely, when the system adapts to odor B, the activation level of $g_B(s)$ becomes very small, and the 50/50 mixture presents a pattern that resembles that of odor A. From the vertical scales in Figure 6, it can also be observed that the algorithm lowers the overall activation levels on both cumulative discriminants as a result of cross-adaptation. Therefore, classification must be performed by considering the ratio of cumulative discriminants rather than their absolute value.

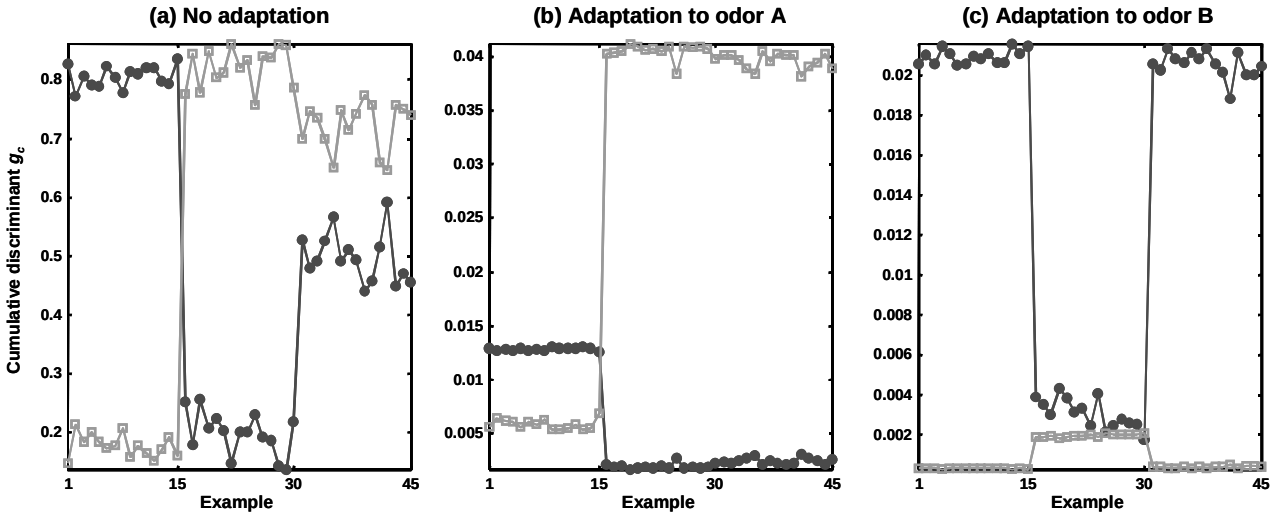

Figure 6. Cumulative discriminant activation g_A (circles) and g_B (squares) for different adaptation scenarios. Examples 1-15 are from odor A, 16-30 are from odor B and 31-45 are from the 50/50 mixture.

6 Conclusions and future work

In this article we have presented an algorithm that mimics the process of chemosensory adaptation in the mammalian olfactory system. The algorithm builds a family of linear discriminant functions that operate on different features vectors (sensor bundles) of the overall sensory input. The relative selectivity of these discriminants determines a set of weighting coefficients for generating cumulative activation levels, which serve as indicator variables for each odor. An inhibitory term is included to reduce the contribution of the different feature vectors, allowing the system to lower its sensitivity to previously detected odors.

The algorithm was evaluated on a dataset of two organic solvents and their 50/50 mixture using an array of four temperature-modulated metal-oxide gas sensors. A larger dataset of three organic solvents and their binary and ternary mixtures is being collected at the time of this writing for further testing of the algorithm. The effect of relative concentrations on the perception of mixtures and on chemosensory adaptation constitutes the next stage of this research. The use of non-linear discriminant functions (e.g. Multilayer Perceptrons or Radial Basis Functions) needs to be evaluated as it may increase the performance of the discriminant functions and, therefore, the ability of the system to adapt its selectivity. Active gas sensing, where the temperature range of each individual sensor is adjusted on-line to reduce sensitivity to previous stimuli, is also a promising extension of this work.

7 Acknowledgments

This research was supported by award from NSF/CAREER 9984426.

8 References

[1] J. W. Gardner and P. N. Bartlett, 1999, Electronic Noses, Principles and Applications, Oxford University Press, Oxford, UK.

[2] G. M. Shepherd, 1998, The synaptic organization of the brain, 4th edition, Oxford University Press.

[3] T.C. Pearce, 1997, "Computational parallels between the biological olfactory pathway and its analogue 'The Electronic Nose': Part I. Biological olfaction", in BioSystems 41, pp. 43-67.

[4] G. M. Shepherd, 1993, "Principles of specificity and redundancy underlying the organization of the olfactory system", in Microscopy Research and technique 24, pp. 106-112.

[5] W. Freeman, 1987, "Simulation of chaotic EEG patterns with a dynamic model of the olfactory system," in Biological Cybernetics 56, pp. 139-150.

[6] Z. Li and J. J. Hopfield, 1989, "Modeling of the Olfactory Bulb and its Neural Oscillatory Processing," in Biological Cybernetics 61, pp. 379-392.

[7] Z. Li, 1990, "A Model of Olfactory Adaptation and Sensitivity Enhancement in the Olfactory Bulb," in Biological Cybernetics 62, pp. 349-361.

[8] Z. Li and J. Hertz, 2000, "Odor recognition and segmentation by a model olfactory bulb and cortex," in Network: Computation in Neural Systems 11, pp. 83-102.

[9] B. Malnic, J. Hirono, T. Sato and L. B. Buck, 1999, "Combinatorial receptor codes for odors", in Cell 96, pp. 713-723.

[10] L. B. Buck and R. Axel, 1991, "A novel multigene family may encode odorant receptors: a molecular basis for odor recognition", in Cell, 85, pp. 175-187.

[11] K. J. Ressler, S. L. Sullivan and L. B. Buck, 1994, "Information coding in the olfactory system: evidence for a stereotyped and highly organized epitope map in the olfactory bulb", in Cell 79, pp. 1245-1255.

[12] R. Vassar, S. K. Chao, R. Sitcheran, J. M. Nuñez, L. B. Vosshall and R. Axel, 1994, "Topographic organization of sensor projections to the olfactory bulb", in Cell 79, pp. 981-991.

[13] J. S. Kauer, 1987, "Coding in the olfactory system," in Neurobiology of Taste and Smell, T. E. Finger and W. L. Silver (eds.), Wiley, New York, pp. 205-231.

[14] D. Schild, 1988, "Principles of Odor Coding and a Neural Network for Odor Discrimination," in Biophys. J. 54, pp. 1001-1011.

[15] K. Ikohura and J. Watson, 1994, The Stannic Oxide Gas Sensor, Principles and Applications, CRC Press, Boca Raton, FL.

[16] J. W. Grate, S. L. Rose-Pehrsson, D. L. Venezky, M. Klusty and H. Wohltjen, 1993, "Smart sensor system for trace organophosphorus and organosulphur vapor detection emplying an temperature-controlled array of surface acoustic wave sensors, automated sample preconcentration and pattern recognition," in Analytical Chemistry 65, pp. 1868-1881.

[17] B. Hivert, M. Hoummady, D. Hauden, P. Mielle, G. Mauvais, and J.M. Henrioud, 1995, "A fast and reproducible method for gas sensor screening to flavour compounds," in Sensors and Actuators B 27(1-3), pp. 242-245.

[18] T. Eklov, P. Martensson and I. Lundstrom, 1997, "Enhanced selectivity of MOSFET gas sensors by systematical analysis of transient parameters," in Analytica Chimica Acta 353, pp. 291-300.

[19] R. Gutierrez-Osuna, H. T. Nagle and S. S. Schiffman, 1999, "Transient response analysis of an electronic nose using multi-exponential models," in Sensors and Actuators B, Chemical, 61(1-3), pp. 170-182.

[20] M. E. H. Amrani, K.C. Persaud and P. A. Payne, 1995, "High-frequency measurements of conducting polymers: development of a new technique for sensing volatile chemicals," in Measurement Science and Technology 6(10), pp. 1500-1507.

[21] U. Weimar and W. Gopel, 1995, "A.C. measurements on tin oxide sensors to improve selectivities and sensitivities," in Sensors and Actuators B 26-27, pp. 13-18.

[22] A. P. Lee and B. J. Reedy, 1999, "Temperature modulation in semiconductor gas sensing," in Sensors and Actuators B 60, pp. 35-42.

[23] M. J. Madou and S. R. Morrison, 1989, Chemical Sensing with Solid State Devices, Academic Press, Boston MA.

[24] R. Gutierrez-Osuna, S. Korah and A. Perera, 2001, "Multi-Frequency Temperature Modulation for Metal-Oxide Gas Sensors," in Proceedings of the 8th International Symposium on Olfaction and the Electronic Nose, Washington, DC, March 25-30, 2001.

[25] Figaro, 1996, General Information for TGS Sensors, Figaro Engineering, Inc., Osaka, Japan.

[26] S. Nakata, E. Ozaki and N. Ojima, 1998, "Gas Sensing Based on the Dynamic Nonlinear Responses of a Semiconductor Gas Sensor: Dependence on the Range and Frequency of a Cyclic Temperature Change," in Analytica Chimica Acta 361, pp. 93-100.